Tests of Storage Rack Channel Columns with Rear Flanges

Nabil Abdel-Rahman

Ashraf Fadel

Mohamed El-Sadaawy

Sherif Mourad

Seventeenth International Specialty Conference on Cold-Formed Steel Structures
Orlando, Florida, U.S.A, November 4-5, 2004

TESTS OF STORAGE RACK CHANNEL COLUMNS WITH REAR FLANGES

Nabil Abdel-Rahman[1], Ashraf Fadel[2], Mohamed. El-Sadaawy[2], and Sherif Mourad[3]

ABSTRACT

An experimental study was performed to investigate the ultimate strength and modes of failure of axially loaded channel rack columns with rear flanges. A total of 16 column specimens fabricated by press-brake forming method were tested up to failure. The material properties of the column specimens were determined using standard tensile coupon tests. The deformation and stress behavior of the tested columns were monitored using displacement transducers and strain gauges. The effects of column slenderness ratio, thickness, perforation, and end conditions on the column ultimate strength and mode of failure were studied. The test failure loads were compared to the ultimate load predictions of the 2001 AISI North American Specification. The comparison showed that the AISI procedure overestimates the failure load, which suggests that the proportioning of the cross-sectional dimensions of the lipped channel sections with rear flanges has a direct effect on the capacity of the columns.

INTRODUCTION

The use of light steel rack systems in storage areas has become widely used due to its low cost, high strength-to-weight ratio, and ease of fabrication and assembly. Pallet racking is one of the most widely used systems, where the

[1] Research & Development, The Steel Network Inc., Raleigh, NC.
[2] Housing and Building Research Center, Giza, Egypt.
[3] Structural Eng. Dept., Faculty of Eng., Cairo University, Giza, Egypt.

racking consists of thin walled compression members and beams with hook-on connectors, as shown in Figure 1. Columns of individual steel storage racks are generally made of cold-formed steel lipped channels. The columns are braced into upright frames by connecting inclined bracing between the channel lips of opposing channels using either welded or bolted connections. If welding is used, the braces are welded directly to the flange stiffening lips. If bolting is used, additional elements parallel to the channel flanges are located at the ends of the flange stiffening lips, and are often used to permit the braces to be bolted to the channel column. These additional elements, called "Rear Flanges", are often wide and may require additional lip stiffeners as shown in Figures 2-a and 2-b. Perforations in these special lipped channel sections are formed by displacing the material of the cross-section by 6 mm as shown in Figure 2-b.

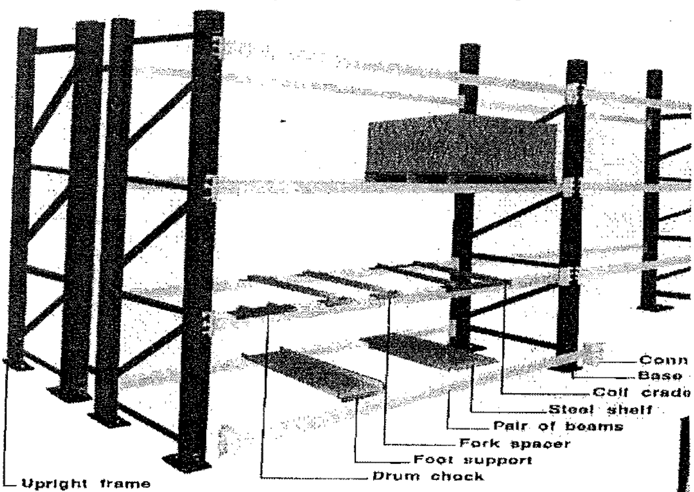

Figure 1: Pallet racking with columns and beams with hook-on connectors

Cold-formed steel columns are vulnerable to local buckling mode at relatively low axial compression loads. Also as columns of storage racks normally have high slenderness ratio, the columns are vulnerable to overall buckling mode, usually referred to as flexural-lateral torsional buckling. This paper investigates experimentally the ultimate strength and modes of failure of axially loaded channel rack columns with rear flanges. The paper also evaluates the experimental test results against predictions of standard codes. A total of 16 column specimens have been tested up to failure. The column specimens were divided into two groups, un-perforated and perforated specimens. The un-perforated group was tested under pinned-pinned end conditions, while the perforated group was tested under both pinned-pinned and fixed-pinned end conditions. The effects of column slenderness ratio, thickness, perforation, and end conditions on the column ultimate strength were studied.

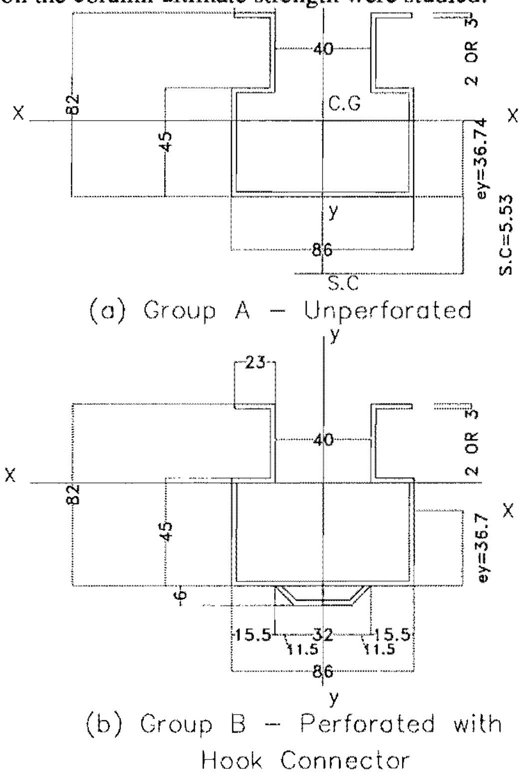

Figure 2: Cross sections and dimensions of column specimens (in mm)

BACKGROUND

Several researchers conducted experimental testing on thin-walled columns. Hancock and Roos (1986) studied the flexural-torsional buckling mode of the columns forming the upright frames of industrial bolted steel storage racks. The tests were designed to produce effective lengths in flexure and torsion, which would be similar to those in full scale frames. The deformation modes of the test frames were found to be similar to the buckling modes computed assuming flexible brace-column joints. Lau and Hancock (1988) tested sixty eight channel columns of different section geometry, length, thickness, and steel grades under uniform compression in a fixed-fixed end condition. It was found that short columns failed mainly by inelastic local buckling, while intermediate length columns failed by inelastic distortional buckling and long columns failed by either elastic or inelastic flexural-torsional buckling. Weng and Pekoz (1990) reported an experimental study of the flexural buckling strength of cold-formed steel columns shaped as lipped channels. A total of 93 columns were tested, focusing on the influence of few parameters affecting the column strength, which included residual stresses, material yielding type, and the forming method used to form the section. The results of the column tests showed that column formulas used in AISI North American Specification (NASPEC, 2001) give un-conservative predictions in some cases. Other experimental work on cold-formed steel channel columns by Miller and Pekoz (1994) and Young and Rasmussen (1998a, 1998b) has also been cited.

The 2001 AISI North American Specification (NASPEC, 2001) provides a method to calculate the nominal capacity of the perforated channel column as a function of the nominal buckling stress of the column F_n and the effective net area calculated at stress F_n. Also, the Specification of the Rack Manufacturers Institute (RMI, 1997) recommends the use of stub-column tests to establish the factor Q and calculate the effective net area of the perforated channel section as a function of the factor Q.

EXPERIMENTAL INVESTIGATION

Preparation of Test Specimens

Experimental testing was conducted on a total of 16 column specimens with two different thicknesses, 2.0 and 3.0 mm (0.079 and 0.118 in.), and two column lengths, 2000 and 3000 mm (80 and 120 in.). The column specimens were divided into two groups: Group A for the un-perforated columns and Group B for the perforated columns. Table 1 summarizes the nomenclature, dimensions, and end conditions of all tested specimens. All the specimens were fabricated by press-brake forming method. The dimensions of the column specimens were measured by a digital micrometer to the accuracy of 0.005 mm (0.0002 in.). Testing was conducted at the Research Laboratory of the Housing and Building Research Center in Giza, Egypt. The cross-sections and nominal dimensions of column specimens are shown in Figures 2-a and 2-b.

Table 1: Dimensions and nomenclature of test specimens

Length (mm)	Thick. (mm)	Group (A)		Group (B)	
		Specimen*	End Cond.	Specimen*	End Cond.
2000	2.0	AU2-L21-P	P-P	BU2-L21-P	P-P
		AU2-L22-P	P-P	BU2-L22-P	P-P
		AU2-L23-P	P-P		
	3.0	AU3-L21-P	P-P	BU3-L22-P	P-P
				BU3-L21-F	F-P
3000	2.0	AU2-L31-P	P-P	BU2-L31-P	P-P
		AU2-L32-P	P-P	BU2-L32-P	P-P
		AU2-L33-P	P-P		
	3.0	AU3-L31-P	P-P	BU3-L31-P	P-P
				BU3-L32-F	F-P

* Specimen nomenclature: (Group No.) U (Thick., mm) - L (Length, m) (Test specimen No.) - (Upper end condition, P for pinned and F for fixed, while lower end was always pinned).

The material properties of the column specimens were determined using standard tensile coupon tests according to the procedure recommended by the ASTM Standard A370-92 (ASTM, 1994) for sheet-type materials. These properties are the yield strength, the ultimate strength, and the modulus of elasticity of the steel. Table 2 lists the resulting material properties of the tensile coupons. Details of the results of the tensile coupon tests are given in El Sadaawy (2003).

Table 2: Material properties of tensile coupons

Column Specimen	Avg. Thick. (mm)	Avg. Yield Strength (MPa)	Avg. Ultimate Strength (MPa)	Modulus of Elasticity (GPa)
Specimens Thick. 2 mm	1.98	311	390	210
Specimens Thick. 3 mm	3.16	324	467	172

Column specimens were cut using a machine saw to the desired length from specimens provided by the manufacturer. Two hot-rolled flat steel plates 200x200x20 mm (8x8x0.789 in.) were welded to the ends of the specimens through 50x50x5 mm (2x2x0.197 in.) angles around the cross-section. To minimize weld-induced distortion, sequential intermittent fillet welds were symmetrically applied on both sides of the section with the connecting angles. Four foil strain gauges were mounted at mid-height of the column specimen at the locations shown in Figure 3. The strain gauges were used for alignment as well as measurement of the strains at each load level using a data logger system.

Specimens Alignment and Measurement Devices

Alignment of the column specimen with the axis of the testing machine is an important step to be performed before running the test. Geometric alignment method was used to align the column specimens. Geometric alignment consists of centering the specimen in the testing machine at its gross centroid. Due to the difficulty of precisely aligning the centroid of the specimen to the center of the machine table, a certain arrangement has been made by using an upper and lower plates connected to the machine and centered with its axis.

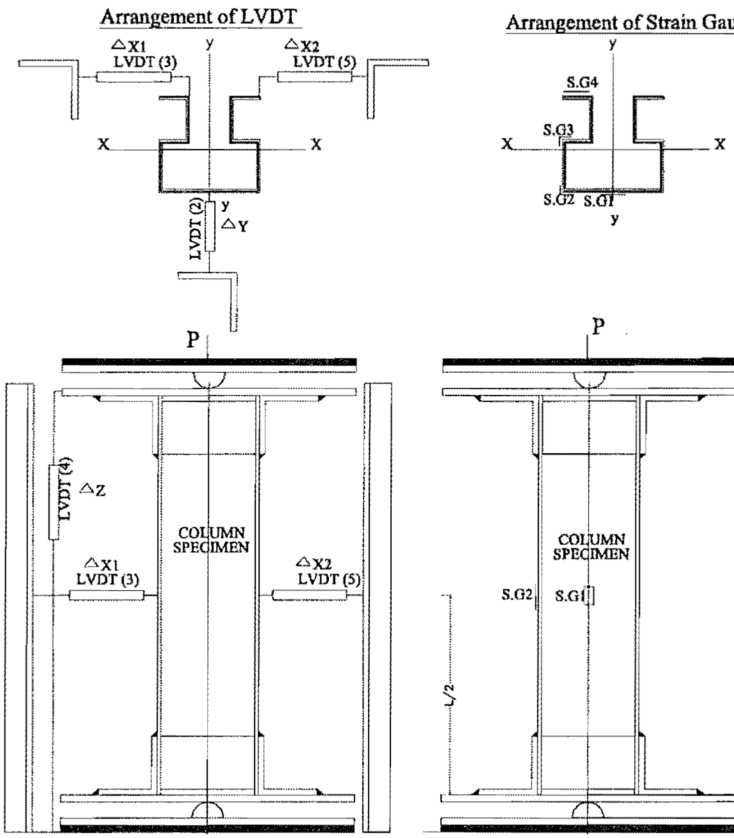

Figure 3: Setup of LVDT and strain gauges for pinned specimens

The end supports of the test specimen consisted of a ball roller at the lower end while the upper end of the column specimen rested on the bearing of the testing machine, which itself rested on a ball bearing to allow rotation in all directions. The ball roller consisted of two parts; one was welded with the plate connected to the machine, while the other part was welded to the end plate column. In the case of fixed-pinned end conditions, the upper head of the column was connected to the upper plate of the machine without the ball roller, but only surrounded by a rod welded to the upper machine plate to ensure the alignment and the verticality of the column. By using this method, the effects of misalignment were minimized, and the behavior of a centrally loaded straight column could be studied more closely.

Displacements of the column specimens during the test were measured using linear variable differential transducers (LVDT). Four sets of transducers were used to measure the displacements in the column tests. The arrangement of the transducers for the pinned-pinned end conditions is shown in Figure 3. LVDT No. 4 was used to measure the axial shortening in the columns Δ_z, while LVDT No. 2 was used to measure the horizontal displacement in the y direction Δ_y. LVDT's No. 3 and 5 were used to measure the horizontal displacement in the x direction Δ_{x1} and Δ_{x2} (distortional). These two transducers were placed at the location where maximum lateral deformation was expected. That location is the mid-height section of the column specimen for the pinned–pinned end conditions. The column specimens with fixed–pinned end conditions had the same strain gauge and LVDT locations, with the exception of LVDT's No. 3 and 5 which were placed at one-third of the height from the loaded end. The displacement transducers were installed after completion of the column alignment. Then, the strain gauges were connected to the data logger system and the loading procedure was employed.

Test Procedure and Results

A 500 kN (112 kips) capacity hydraulic testing machine, along with a data acquisition system, was used for testing the column specimens. The axial compression load was applied in small increments. The load increment was varied according to the expected failure load of the column. The load increment did not exceed 10% of the expected failure load, or 10 kN (2.2 kips), whichever was less until reaching 50% of the expected failure load. Beyond this point, the load increment was reduced to 5% of the expected failure load, or 5 kN (1.1 kips), whichever was less. Readings of the displacement transducers and the electric strain gauges were recorded at each load increment. Failure of the column specimens was marked by the start of the drop in the applied load readings. However, some specimens were continued to be loaded in compression to exaggerate the failure deformation shape. Figure 4 shows a sample flexural buckling failure around x-axis.

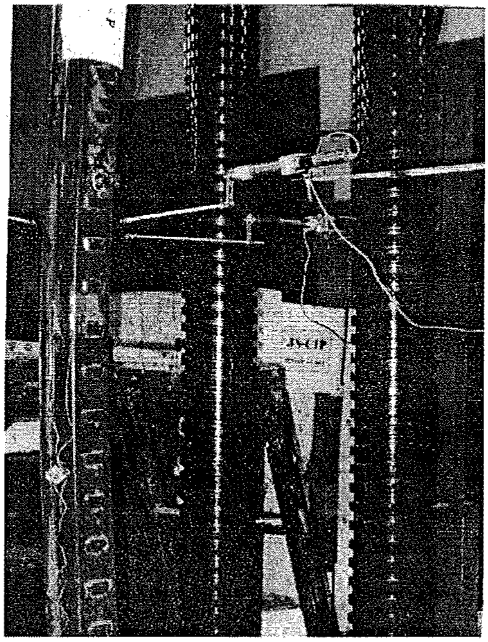

Figure 4: Distortional flexural buckling failure mode around x axis

Table 3 shows the failure loads of all column specimens. The column specimens AU2-L21-P and AU2-L32-P experienced an undesired impact load at the start of the test, which adversely affected the strength of the columns. However, the load results of these specimens were taken into consideration in the analysis. The relationships between the applied load with the axial shortening Δ_z and the lateral displacement Δ_y are shown in Figure 5 for column specimens of thickness 2 mm (0.079 in.) and in Figure 6 for column specimens of thickness 3 mm (0.118 in.), respectively.

Table 3: Experimental and AISI Specification ultimate loads

Group	Specimen	Experimental: Failure Load P_t (kN)	Experimental: Avg. P_t (kN)	AISI (2001): P_{AISI} (kN)	P_t/P_{AISI}
(A) Un-perforated	AU2-L21-P	102.5	126.0	150.0	0.840
	AU2-L22-P	138.3			
	AU2-L23-P	137.1			
	AU3-L21-P	168.2	168.2	217.9	0.772
	AU2-L31-P	110.4	100.5	105.1	0.956
	AU2-L32-P	83.7			
	AU2-L33-P	107.5			
	AU3-L31-P	131.8	131.8	152.2	0.866
(B) Perforated	BU2-L21-P	100.5	102.3	124.6	0.821
	BU2-L22-P	104.1			
	BU3-L22-P	142.9	142.9	179.1	0.798
	BU3-L21-F	190.0	190.0	207.4	0.916
	BU2-L31-P	72.3	72.5	87.0	0.833
	BU2-L32-P	72.8			
	BU3-L31-P	104.0	104.0	125.1	0.832
	BU3-L32-F	160.1	160.1	173.9	0.921

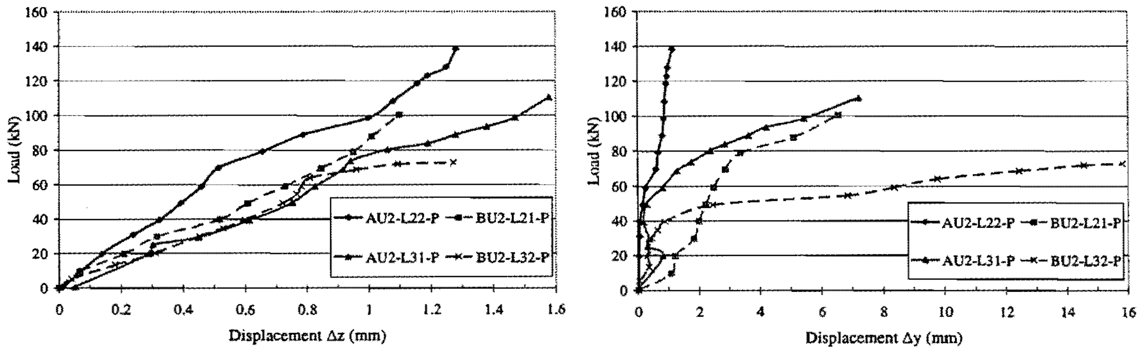

Figure 5 a, b: Axial shortening Δ_z and lateral displacement Δ_y of column specimens of thickness 2 mm

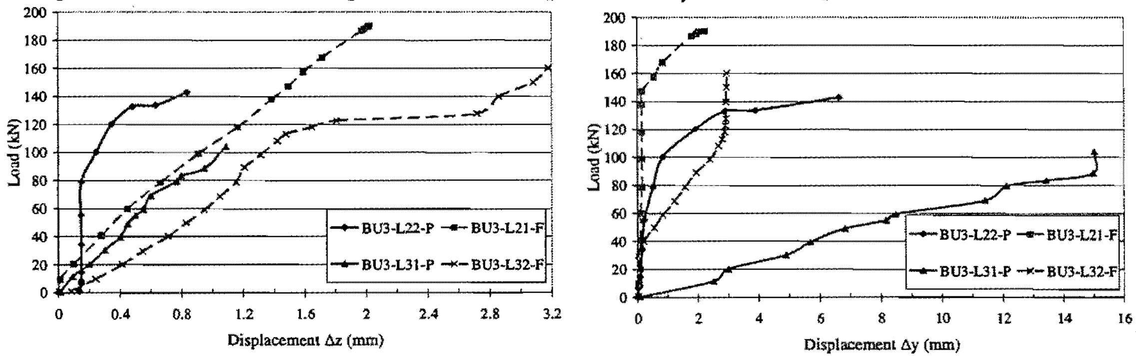

Figure 6 a, b: Axial shortening Δ_z and lateral displacement Δ_y of column specimens of thickness 3 mm

DISCUSSION OF EXPERIMENTAL RESULTS

Failure Loads and Modes of Failure

Experimental failure loads from the current tests are presented in Table 3. The results show that perforated column specimens (Group B) failed at lower loads compared to un-perforated specimens (Group A). The percentage loss in strength due to the perforation was maximum at 28% between specimen series AU2-L3-P and BU2-L3-P, and was minimum at 15% between specimens AU3-L21-P and BU3-L22-P. The experimental results also show that column specimens with fixed-pinned end conditions achieved higher failure loads compared to specimens with pinned-pinned end conditions. This comparison was performed only for perforated column specimens (Group B) of thickness 3 mm (0.118 in.). The load increase due to the fixation at the top end of the specimens was about 33% for specimen BU3-L21-F over specimen BU3-L22-P, and about 54% for specimen BU3-L32-F over specimen BU3-L31-P.

The first noticeable mode of failure of tested column specimens was the distortional-flexural buckling about the x axis for specimens with length 2000 mm (80 in.) for both perforated and un-perforated sections. The second mode of failure was the flexural buckling about x axis for specimens with length 3000 mm (120 in.) for both perforated and un-perforated sections. The third mode of failure was the torsional–flexural buckling about the y axis. This mode occurred unexpectedly in three column specimens AU2-L21-P, AU3-L21-P, and AU3-L31-P.

Deformation Behavior

Figure 5-a shows the relationship between the applied load and the axial shortening of column specimens with thickness 2 mm (0.079 in.). The slope of the line is a representation of the axial stiffness of the column. All specimens in this figure have pinned-pinned end conditions. The figure shows that the initial stiffness of perforated specimen BU2-L21-P, length 2000 mm (80 in.), is less than the initial stiffness of the corresponding un-perforated specimen AU2-L22-P. This is mainly due to the fact that the local buckling stress of perforated sections is less than the corresponding stress of un-perforated sections. Beyond this load, axial stiffness of both the perforated and un-perforated specimens became almost equal due to the initiation of column flexural buckling mode. The column specimens AU2-L31-P and BU2-L32-P, length 3000 mm (120 in.), show similar axial stiffness behavior. Figure 5-b shows the relationship between

the applied load and the lateral displacement Δ_y. Specimen BU2-L32-P shows the most lateral displacement in y direction due to the flexural buckling failure around x axis and the existence of the perforation. Specimen AU2-L22-P shows limited lateral displacement in y direction as it failed mainly in a distortional buckling mode.

Figure 6-a shows the relationship between the applied load and the axial shortening of column specimens with thickness 3 mm (0.118 in.). All specimens in this figure are perforated specimens (Group B). The figure shows that specimens with one fixed end and one pinned end (BU3-L21-F and BU3-L32-F) experienced lower axial stiffness than the corresponding specimens with pinned end at both sides (BU3-L22-P and BU3-L31-P, respectively). An explanation for this behavior is that the fixed condition at the loaded end of the specimens limited the lateral displacement of the specimens and caused a build-up of axial stresses in the column. This resulted in the local buckling stress to be reached in these specimens early in the loading process. This conclusion can be confirmed by checking the lateral displacement behavior in Figure 6-b. In this figure, column specimens with fixed-pinned end condition experienced very limited lateral displacement in y direction compared to the corresponding specimens with pinned-pinned end conditions.

Comparison to AISI Specification Predictions

The ultimate loads predicted by the AISI Specification (NASPEC, 2001) for the column specimens are presented in Table 3. For the perforated specimens, the web plate containing the perforation was treated as two un-stiffened plates according to AISI recommendations. The effective length factor of the column specimens was taken equal to 1.0 for pinned-pinned end conditions and equal to 0.7 for fixed-pinned end conditions. The comparison of the AISI predicted ultimate loads to the test failure loads shows that test loads are consistently less than the AISI predicted loads. The difference between the test results and the AISI results can be as large as 23%. This finding is similar to the findings presented by Weng and Pekoz (1990) for about 50 lipped channel column tests. This suggests that the proportioning of the cross-sectional dimensions of the current-used lipped channel sections with rear flanges may have a direct effect on the capacity of the columns. Although AISI column equations were developed as the best fit of hundreds of column tests, the current channel cross-section under consideration may require special attention to develop an appropriate set of design equations. The AISI results of the two column specimens with fixed-pinned end conditions (BU3-L21-F and BU3-L32-F) show better correlation with the test results than the other specimens with pinned-pinned end conditions.

CONCLUSIONS

The current experimental study was performed to investigate the ultimate strength and modes of failure of axially loaded channel rack columns with rear flanges. Sixteen column specimens with different length, thickness, and end conditions were tested. The test results showed that columns with web perforations experienced lower axial stiffness and failed at lower loads compared to un-perforated columns. The loss in strength due to the perforation ranged between 15% and 28%. Columns with fixed-pinned end conditions achieved higher failure loads compared to columns with pinned-pinned end conditions by up to 54%. As for modes of failure, columns with length 2000 mm (80 in.) generally failed in distortional-flexural buckling mode, while columns with length 3000 mm (120 in.) failed in flexural buckling mode. Comparison of AISI predicted ultimate loads to the test failure loads showed that test loads are consistently less than the AISI predicted loads. The un-conservative nature of the AISI load predictions suggests that the proportioning of the cross-sectional dimensions of the lipped channel sections with rear flanges has a direct effect on the weakening of the columns.

REFERENCES

ASTM Standards (1994), "Standard Test Method and Definitions for Mechanical Testing of Steel Products", American Society for Testing and Materials, A370-92, Philadelphia, USA.

El Sadaawy, M. M. (2003), "Elasto-Plastic Analysis and Experimental Testing of Cold-Formed Perforated and Unperforated Steel Storage Rack Columns", Ph.D. Thesis, Department of Structural Eng., Faculty of Eng., Cairo University, Giza, Egypt.

Hancock, G.T. and Roos, O. (1986), "Flexural-Torsional Buckling of Storage Rack Columns", Proceeding of the 8th International Specialty Conference on Cold-Formed Steel Structures, University of Missouri-Rolla, USA.

Lau, S.C.W. and Hancock, G. T. (1988), "Tests of Cold-Formed Channel Sections", Proceeding of the 9th International Specialty Conference on Cold-Formed Steel Structures, University of Missouri-Rolla, USA.

Miller, T. and Pekoz, T. (1994), "Load-Eccentricity Effects on Cold-Formed Steel Lipped-Channel Columns", Journal of Structural Engineering, ASCE, Vol. 120, No. 3.

NASPEC (2001), "North American Specification for the Design of Cold-Formed Steel Structural Members", American Iron and Steel Institute Standard, 2001 Edition, Washington, D.C., USA.

RMI (1997), "Specification for the Design, Testing and Utilization of Industrial Steel Storage Racks", Rack Manufacturers Institute, USA.

Weng, C.C. and Pekoz, T. (1990), "Compression Tests of Cold-Formed Columns", Journal of Structural Engineering, ASCE, Vol. 116, No. 5.

Young, B. and Rasmussen, K.J.R. (1998a), "Design of Lipped Channel Columns", Journal of Structural Engineering, ASCE, Vol. 124, No. 2.

Young, B. and Rasmussen, K.J.R. (1998b), "Tests of Fixed-Ended Plain Channel Columns", Journal of Structural Engineering, ASCE, Vol. 124, No. 2.

APPENDIX: NOTATIONS

F_n = Nominal buckling stress.

Δ = Displacement, axial or lateral.

P_t = Ultimate test load.